# Modification of the Natural Photonic Bandgap of Synthetic Opals via Infilling with Crystalline InP**

By *Heather M. Yates*,* *Martyn E. Pemble*, *Elisa Palacios-Lidón*, *Florencio García-Santamaría*, *Isabelle Rodriguez*, *Francisco Meseguer*, and *Cefe López*

The growth of high-quality stoichiometric indium phosphide by atmospheric pressure metal–organic chemical vapor deposition within thin-film artificial opals has been optimized. The optical properties of these systems have been studied as a function of the filling fraction. A consistent behavior has been found which substantially differs from that of other common infilled opals. The evolution of the InP morphology seems to be strongly correlated with this anomalous photonic response. At the first infiltration stages, the growth leads to the formation of nanocrystallites that eventually, as the infiltration increases, coalesce in single-crystalline grains of increasing size. The possibility to oxidize the material adds to its potential as a useful optical material.

## 1. Introduction

Since the pioneering work of Yablonovich et al.[1] and John[2] there has been an enormous amount of interest in the fabrication and study of the so-called photonic-bandgap (PBG) materials, also known as photonic crystals. This kind of system can be used to control light propagation in a way analogous to what semiconductors do with electrons.[3] The synthesis of synthetic opals[4] and related polymer systems provides a potentially cheap and effective means of creating three-dimensional (3D) photonic structures.[5] By the self-assembly of silica ($SiO_2$) or spherical polymer colloids in a close-packed face-centered cubic lattice, large samples (on the order of square millimeters) with a well-defined optical response can be obtained. Subsequent to growth, these porous systems may be modified via infilling with materials of high refractive index. In this way their photonic properties are significantly enhanced because of the resulting increase in refractive-index contrast as compared to the bare sphere–air host structure.[6] Once the sphere matrix is removed, the inverse structure is obtained. If the refractive index of the infilled material is high enough ($>2.8$), then a full PBG is opened between the eight and ninth bands.[7,8] Indeed, some inverse opals showing such a refractive-index contrast and behavior have been reported.[9–11]

Indium phosphide (InP) is a particularly interesting material as it possesses a direct electronic gap, thus, the fabrication of InP–opal composites or InP inverted-opal structures opens up the possibility of fabricating a photonic structure from a medium that is itself capable of efficient light emission.[12] Therefore, the ability to fabricate such materials is an important milestone in the drive towards integration of photonic-bandgap technologies with conventional semiconductor processing methods.

Although much work has concentrated on bulk opals, only a small number of layers are actually required for photonic behavior.[13,14] Thus, a further milestone which remains to be achieved is the successful fabrication of thin-film III–V semiconductor/opal composites with well-defined optical responses, rather than bulk structures. Significant progress has already been made in terms of methods designed to fabricate high-quality, thin-film opaline structures.[15–17] In particular, methods which allow deposition of opal structures directly onto Si, or another semiconductor,[18] go some considerable way towards demonstrating the possibility of integrating Si chip technology with that of opaline photonic devices.[19,20]

In recent studies we have show the possibility of infilling silica opals with III–V materials (InP and GaP) by using metal–organic chemical vapor deposition (MOCVD) methods.[21] These methods have proven to be successful, so it was also possible to produce the first examples of III–V inverted-opal structures (Fig. 1). The photonic response of the composites $InP/SiO_2$ structures was anomalous, showing an apparent very-small-to-non-existent shift in the Bragg peak. In the case of inverted structures, even a shift to lower wavelength was observed (this result would imply an impossible negative refractive index or negative filling fractions), accompanied by the appearance of intense peaks at higher energies.

[*] Dr. H. M. Yates, Prof. M. E. Pemble[+]
Institute for Materials Research, Cockcroft Building
University of Salford
Salford, M5 4WT (UK)
E-mail: h.m.yates@salford.ac.uk
E. Palacios-Lidón, F. García-Santamaría,[++] Dr. C. López
Instituto de Ciencia de Materiales de Madrid (CSIC)
C/Sor Juana Inés de la Cruz, 3, E-28049 Madrid (Spain)
Prof. F. Meseguer, Dr. I. Rodriguez
Unidad Asociada CSIC-UPV
Avenida de los Naranjos s/n, E-46022 Valencia (Spain)
[+] Present address: NMRC, Lee Maltings, Prospect Row, Cork, Ireland.
[++] Present address: Department of Materials Science and Engineering, Beckman Institute for Advanced Science and Technology and Frederick Seitz Materials Research Laboratory, University of Illinois at Urbana-Champaign, 1304 West Green St., Urbana, IL 61801, USA.

[**] This work is partially financed by the European Commission through IST-1999-19009 PHOBOS project and Spanish MEC through MAT 2003-01237 project. E. Palacios-Lidón thanks Comunidad Autónoma de Madrid for a predoctoral grant.

 DOI: 10.1002/adfm.200400248  

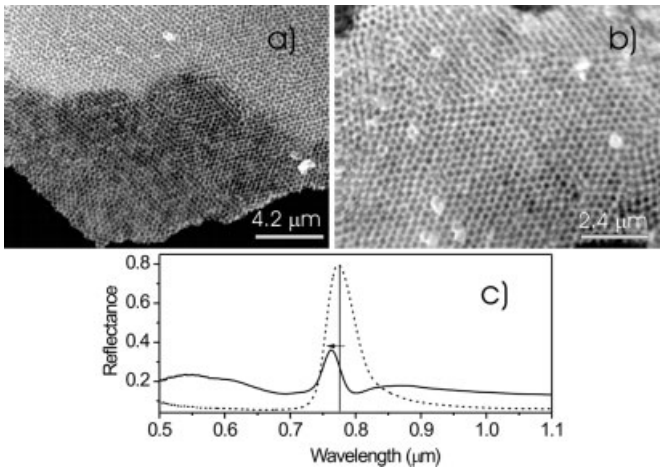


**Figure 1.** a) SEM image of an InP inverse opal, large area. b) Magnified detail of (a). c) Reflectance spectrum of the original composite InP/silica opal (solid line) compared with the bare silica opal (dash line). The anomalous photonic response is evident.

Here, we present a detailed study of the characterization of InP infiltration (using a modified MOCVD method) in thin-film silica opals grown using the vertical deposition method.[15] The main aim was to confirm that the material grown was high-quality crystalline InP, so that any unexpected optical behavior could be imputed not to a failure in the growth, but to some other cause yet to be found. Since the behavior has been found to be consistent regardless of specific sample preparation details, we consider this to be an intrinsic effect for this material. In addition, the sphere size (660 nm) has been chosen in order that the photonic properties lie out of the InP absorption zone, ensuring that these anomalous features are not due to a complex dielectric function.

To study the growth evolution, a series of samples with differing amounts of infilled InP was prepared by increasing the number of deposition cycles. It is confirmed that increasing numbers of cycles lead to increasing degrees of InP infiltration. We have found that, after a threshold filling fraction is exceeded, the photonic response of the system suddenly changes its behavior, presenting features which cannot be, even qualitatively, explained by a simple Bragg-diffraction analysis. We suggest that the most likely explanation of this behavior, noting that the optical response appears to be directly related to the morphology of the infill, which is also seen to vary with the extent of infiltration, is, precisely, a sudden change in the morphology of the compound grown at a certain filling fraction.

## 2. Results and Discussion

The characterization and analysis will be discussed in two sections. Firstly, we focus our attention on studying the composition and morphology of the InP placed within the opal voids. Secondly, we concentrate on the optical characterization, which has been done by means of reflectance spectroscopy. As the optical measurements are strongly dependent on the infill material properties, we have tried to find a direct relationship between the results.

Four samples have been prepared with differing levels of infill, from low infill (sample A) to high infill (sample D) as shown in Table 1. It is important to note that the infiltration value given is just an estimate taken from scanning electron microscopy (SEM) images and optical measurements. As will be shown, in this kind of composite system it is difficult to obtain an absolute filling fraction for the highly infiltrated samples.

**Table 1.** Sample name and estimated infiltration (percentage of volume) of the sample series (see text).

| Sample | Estimated infiltration [%] |
|---|---|
| A | 4 |
| B | 10 |
| C | 26 |
| D | 50 |

Raman spectroscopy analysis (Fig. 2) shows that good-quality polycrystalline InP has been achieved. In the Raman spectra, the bands located at 303 $cm^{-1}$ and 340 $cm^{-1}$ can be assigned to transverse-optical (TO) and longitudinal-optical (LO) normal modes of InP respectively, in agreement with the bulk values reported in the literature ($\nu_{TO} = 304$, $\nu_{LO} = 345$ $cm^{-1}$).[22]

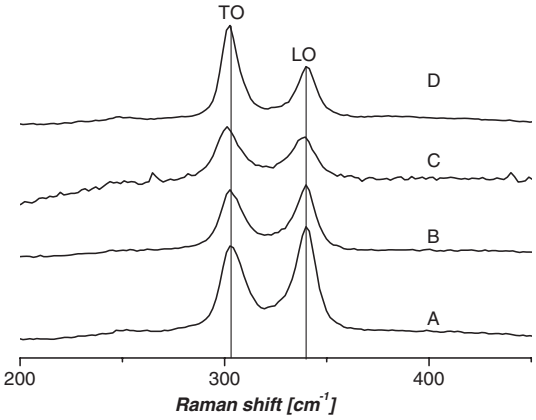


**Figure 2.** Raman spectra of various InP/opal thin films. TO and LO refer to the transverse-optical and longitudinal-optical normal modes, respectively.

The X-ray diffraction (XRD) patterns (Fig. 3) show the presence of stoichiometric, crystalline InP (cubic $\tilde{F}4m$(216) phase). Further analysis of the XRD patterns using Rietveld methods[23] allows the refinement of several structural parameters including lattice constant ($a_0$), domain size, cell strain, and preferential orientation following the March–Dollase method (Table 2). The lattice parameter of the deposited InP is slightly lower than that of bulk InP (5.869 Å). Additionally, from the relative intensity of the peaks it is possible to determine that the InP grains grow preferentially oriented with the (111) di-

  

ADVANCED FUNCTIONAL MATERIALS



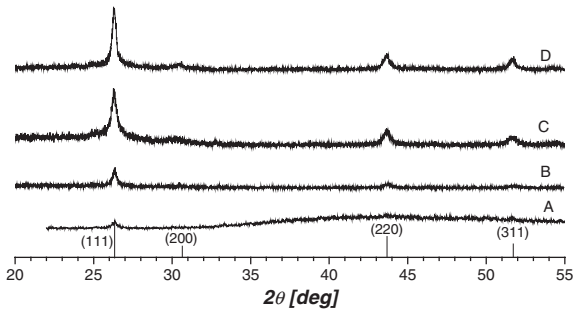


**Figure 3.** XRD patterns of InP/opal thin films.

**Table 2.** Details of Rietveld analysis: lattice constant ($a_0$), domain size, lattice strain, and March–Dollase parameter.

| Sample | $a_0$ [nm] | Domain size [nm] | Strain | M–D along (111) |
|---|---|---|---|---|
| B | 0.5855 | 19 | 0.00078 | 0.58549 |
| C | 0.58614 | 37 | 0.0036 | 0.58614 |
| D | 0.584 | 56 | 0.005 | 0.5840 |

rection perpendicular to the opal surface. However, the most relevant information is obtained from the crystalline domain size, which drastically increases (from 19 to 56 nm) as the degree of infiltration rises. This result is consistent with the increase in the lattice strain. From the X-ray study it may be concluded that in the growth process the material tends to form larger grains preferentially oriented along the (111) direction instead of increasing the density of small grains with random orientation at the surface of the spheres. No analysis was possible for sample A due to the low concentration of InP within the opal pores which produces too small an XRD signal. This signal becomes more intense as the amount of InP increases.

The evolution of the samples infiltration is confirmed by SEM inspection. An image of bare opal is also shown (Fig. 4a) for comparison with the infilled opals. At low infiltration (Fig. 4b), it is possible to see small grains on the spheres' surfaces. As the infiltration increases, the spheres become completely covered by small grains (Fig. 4c). When the amount of InP deposited is high, the pores begin to close up (Fig. 4d).

By comparing magnified areas for different infill samples (Fig. 5), a detailed study of the grain morphology confirms the previously noted grain-growth tendency. For low infiltration (Fig. 5a), small, independent grains a few tens of nanometers in size are clearly distinguished on the spheres' surfaces, in contrast to the high-infiltration situation (Fig. 5b), where large grains appear (~50 nm or larger). The grains themselves are now barely discernible because, as the infiltration proceeds, they start to coalesce and a continuous material is formed from independent grains.

From the results from XRD, Raman spectroscopy, and SEM, it can be concluded that the crystallographic structure of the InP deposited is the same, regardless of the degree of infiltration. However, the morphology behaves differently: at low infiltration it consists of nanocrystals on the spheres surface evolving into large grains at high infiltration.

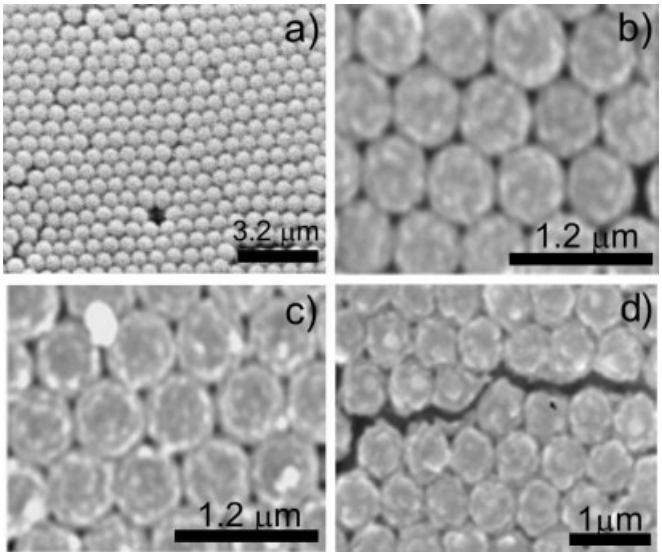


**Figure 4.** SEM images of various stages in the infiltration process. a) Bare opal. b) Sample A (low infilling fraction): small grains covering the spheres. c) Sample C (medium filling fraction): the spheres are completely covered by the InP grains. d) Sample D (higher infiltration): the InP the voids between spheres are nearly closed.

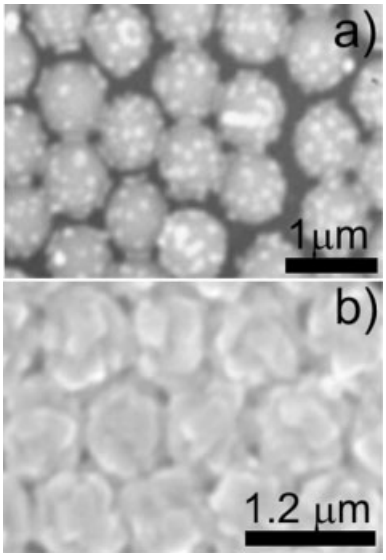


**Figure 5.** Two growth modes: SEM images showing a) the small InP grains over the opal spheres in low infiltration stages and b) extended grains in highly loaded opals.

Optical characterization was carried out by measuring specular reflectance from both bare and infiltrated samples. For this to be successful it is important to make sure that there is no InP thin film covering the sample as a whole, since that would strongly alter the measurements. With this in mind, the tested zones were previously inspected by optical microscopy using a 100× microscope objective. At this magnification, spheres can

  

be clearly distinguished, as seen in Figure 6, which shows an optical microscopy photograph of a sample with medium filling fraction (26 % of the pore volume). It is important to highlight here that it is due to the infiltration that any features at all can be appreciated when using optical microscopy. In the case of bare opals, scattering at the surface of the spheres and at lattice defects produces a high level of stray light that blocks observation, allowing only a blaze of white light to be seen. InP absorption, and probably the high refractive index, helps in imaging the opal lattice. This has also been observed for other absorbing and highly refractive materials such as silicon.[9]

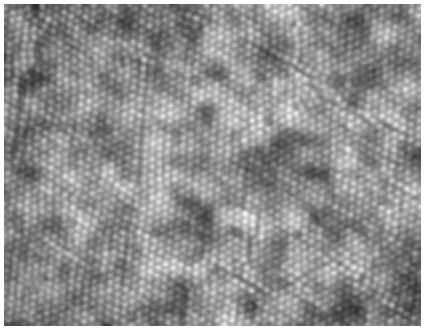

**Figure 6.** Optical microscopy photograph (low magnification) of an InP-infilled opal sample revealing the ordered opal spheres.

In Figure 7a, the evolution of the first pseudo-gap position with the filling fraction is extracted from the band structure obtained using the MPB package,[24] which was developed at Massachusetts Institute of Technology (MIT), based on an iterative plane-wave expansion method. It is worth mentioning that the band-structure calculations have been carried out for a layered infiltration model, which assumes that each silica sphere is covered with a shell of a high refractive index material, while air fills the pores in the interparticle voids. As the infiltration increases, the shell thickness also increases.[25] The calculated results are different from those obtained by assuming a homogeneous infiltration model, in which the pores are completely filled with a medium that densifies with infiltration, and which uses a mean refractive index, taken as a weighted average of the air and the filling material. Although results from the two models agree for very high and very low infiltration, for intermediate values, the results obtained are largely different. In our case, for low infiltrations, SEM images reveal that InP grains are covering the opal spheres; there is consequently no doubt that the layered model is the correct one to be applied. This assumption is further supported by the fact that for infiltrations of a few percent of the pore the thickness of the layer needed to be infiltrated is only of a very few percent of sphere radius which equals some tens of nanometres or one grain size. For the sphere size used (660 nm) the Bragg peak is expected at wavelengths which lie in the transparency region of the infill material so the absorption is negligible and the refractive index can be taken as constant and equal to 3.1.[26]

Comparing this theoretical evolution with the experimental one we can see that the bare-opal spectrum (Fig. 7b) shows a well-defined, intense Bragg peak and Fabry–Perot (FP) oscillations, which are due to the finite thickness of the sample. The period of the FP oscillations relates to the film thickness and also to the effective refractive index of the composite material following:

$$m\lambda = 2dn_{\text{eff}} \tag{1}$$

where $d$ is the film thickness, $n_{\text{eff}}$ the effective refractive index of the system, and $m$ is an integer. To do a complete analysis, the period of oscillation from the infilled samples is compared to that of its corresponding bare opal. If $n_{\text{eff}}$ of the bare opal is calculated using the Maxwell–Garnet approximation[27] (which is customary being granted by the fact that the refractive index

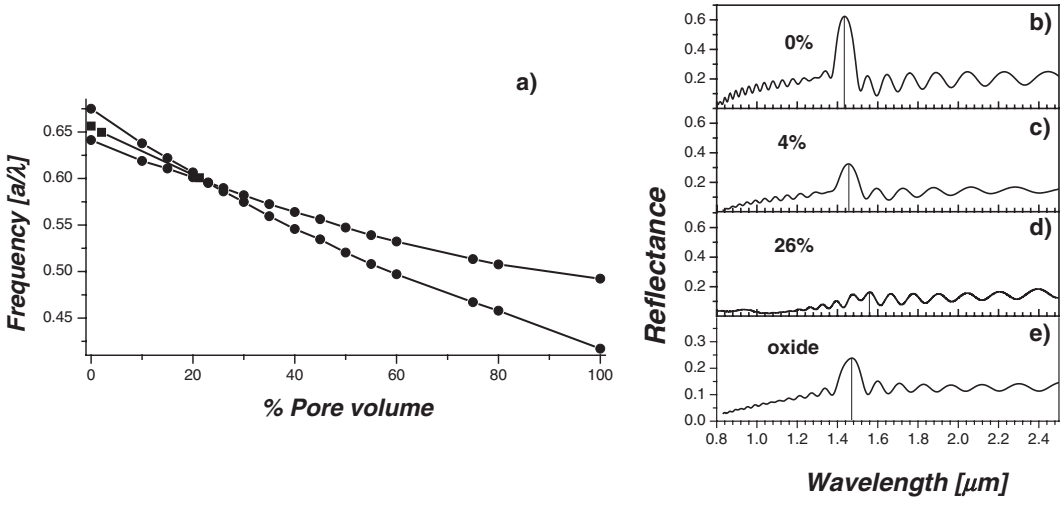


**Figure 7.** a) Evolution of the first pseudo-gap in the (111) direction with the InP filling fraction obtained from the band structure using a layered model. b) Reflectance spectra of a bare thin-film opal. c) Sample A (infilling 4 % of the pore volume). d) Sample C (infilling 26 %). The Bragg peak disappears (index matching). e) Oxidized InP-infilled opal (sample C after oxidation).

  

ADVANCED FUNCTIONAL MATERIALS



of silica is moderate), then it is possible to determine the sample thickness. By assuming the same thickness before and after the infiltration, it is possible to obtain a value for the effective refractive index of the composite structure (Table 3). All the thin-film opal samples are between sixteen and nineteen layers. As expected, the effective refractive index increases with the InP infill. Comparing these results with the refractive index calculated from the slope of the band ($k \rightarrow 0$) an estimation of the filling fraction can be obtained, finding good agreement with SEM observations.

**Table 3.** Sample thickness, number of layers, effective refractive index from FP oscillations analysis ($n_{\text{eff}}$), increase of the refractive index with respect to the bare opal ($\Delta n_{\text{eff}}$), and refractive index extracted from the bands ($n_{\text{bands}}$).

| Sample | Thickness [μm] | Thickness (layers) | $n_{\text{eff}}$] | $\Delta n_{\text{eff}}$ | $n_{\text{bands}}$ |
|---|---|---|---|---|---|
| A | 9.7 | 19 | 1.3 | 0 | 1.300 |
| B | 8.1 | 16 | 1.33 | 0.03 | 1.335 |
| C | 9.7 | 19 | 1.416 | 0.116 | 1.434 |

As expected, at low infiltration (Fig. 7c), the Bragg peak shifts to higher wavelength while the refractive index of the composite opal rises.[28] As the infiltration further increases, a point is reached (Fig. 7d) where no Bragg peak is observed; instead, only FP oscillations are seen. This is occurring because for this degree of infiltration, the effective refractive index of the pores (air plus InP) very nearly matches that of the silica spheres.[25] For this condition, the periodic variation of the refractive index is such that, for this particular wavelength, the material probed is nearly homogeneous and, hence, the Bragg peak associated with internal periodicity is indistinguishable from the rest of the fringes. It is, however, interesting to note that the periodic nature of the sample can be probed by shorter wavelengths that show the features related to the fifth and ninth bands. By using the MPB package, the band structure of the system can be obtained; it is predicted that the Bragg peak is almost closed for a pore-filling fraction of ~26 % (Fig. 8a). However, after the InP oxidation (500 °C for 2 h in air), mainly $InPO_4$ and $In_2O_3$ are formed,[29] the net effect being that silica spheres with a refractive index of 1.43 are now surrounded by a shell of very much the same index (~1.49) without a change of lattice parameter. In this situation, the Bragg peak reappears at the expected position (Fig. 7e) because index matching may no longer occur.[25] As the InP oxides cover the spheres' surfaces and their refractive index is close to that of the silica the resulting spectrum looks similar to that of a sintered opal. That is, it resembles an opal with a filling higher than — or a lattice parameter ($a < D\sqrt{2}$) less than — that for close-packed spheres, but still a silica/air structure with dielectric contrast. This fact is also confirmed by comparing the experimental spectrum with the band-structure calculations (Fig. 8b).

In ordinary infiltrated opal systems, if the infiltration continues increasing beyond the index-matching condition, the Bragg peak reappears moving to higher wavelengths. In the InP-infilled opals for very high infiltration (sample D), this trend is disrupted (Fig. 9).

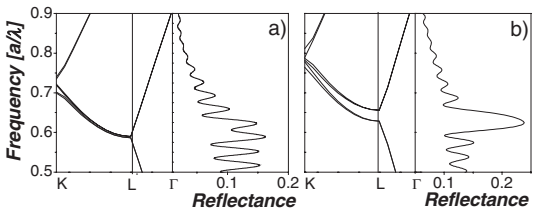


**Figure 8.** a) Experimental InP ($n = 3.1$) thin-film opal compared with band calculation (infilling 26 % pore volume). From this figure it can be seen that the first pseudo-gap at the L point is nearly closed. b) Same calculations as (a) for the oxidized sample ($n = 1.49$) show that at the L point the first pseudo-gap is still open. In both cases the theoretical band structure agrees fairly well with the features observed experimentally.

A sharp peak in much the same position as that for the bare opal and two intense peaks at higher energies are evident. If the filling fraction is calculated assuming this sharp resonance is the first pseudo-gap peak, from its relative shift with respect to the bare opal, and using the laminar model, a filling fraction of less than 1 % is obtained. Analysis of the FP oscillation period also indicates a large increase in the effective refractive index of the system, with $\Delta n_{\text{eff}} = 0.9$. From the layered model this would mean a filling fraction of nearly 100 %, which is in complete contradiction to the Bragg-peak position found. The evidence from XRD, Raman spectroscopy, and direct SEM observation show that although quite a lot of InP is present in the pores, the opal is not fully infiltrated as the pores are still not closed. Therefore, both calculations on the peak position and on the oscillations give wrong results. The only apparent difference during the infiltration process is the change of the grain morphology, which seems to be strongly related to the anomalous optical behavior. It has been shown recently[30] that changes in the morphology of the infiltrated material can produce strong modifications in the band structure, opening and closing the photonic bandgaps, even while the symmetry of the system does not change and, of course, modifying the effective refractive index of the system by changing the bands slopes.

The same anomalous behavior has been found in highly infiltrated thick sedimented opals (not shown). This supports the

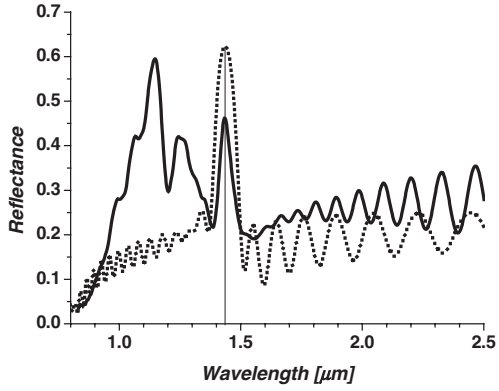


**Figure 9.** Reflectance spectrum (solid line) of a highly infiltrated sample (sample D). The bare opal spectrum (dashed line) has been included to show that there is no appreciable shift with respect to the infiltrated opal.

  

experimental results presented here and shows that this is a reproducible behavior. The experimental procedure used to infill was very similar to that used here for the thin film opals, again using an increasing number of cycles to fully fill the sample. The bulk samples are more easily infiltrated, in as much as reactant gases can be passed straight through the porous opal structure, unlike that of the thin samples, which are deposited on a non-porous silicon substrate. Thus the growth process is much slower, which favors the growth of larger grains.

## 3. Conclusions

This work demonstrates that the fabrication of thin-film photonic devices based upon colloidal assemblies such as opals is indeed a viable technology. Good-quality InP, as seen using XRD and Raman spectroscopy, has been grown inside thin-film opals. From SEM characterization it is possible to see that the degree of infiltration clearly increases with repeated MOCVD cycles. At low infiltration, InP grains cover the opal spheres, confirming that the layered model can be applied in our case. This explains the index-matching effect that is apparent at 26 % of the pore volume and can be proved by oxidizing the sample. When the filling fraction reaches a certain value the optical properties drastically change from the ideal infiltration trend. This behavior is systematic and scales with the size of the spheres. Although no satisfactory explanation can be given at this point, it is proposed that this might be due to the morphology of the material. A deeper understanding of this kind of systems is of vital importance and will be the subject of future work.

We have shown the feasibility of filling opaline systems with conventional III–V semiconductors, using equipment which, apart from the reactors themselves, are "industry standards", and this is a major technological breakthrough. The importance of considering possible chemical and physical changes, in this case the role of oxidation, in thin layer opal systems has been highlighted. Such considerations should be kept in mind in designing photonic-bandgap devices based upon opaline thin films.

## 4. Experimental

The silica spheres were synthesized following the Stöber–Fink–Bohn method [31]. Thin-film opals were grown by means of a convective self-assembly deposition method [15]. A clean silicon substrate is placed vertically in a vial containing a suspension of silica spheres in ethanol, and kept at room temperature for 24 h [25].

The experimental method used for infiltration is that which we have successfully used previously to infill bulk opal [21]. The composite structures are grown in a standard atmospheric MOCVD reactor (Electrogas Systems). The only modification necessary was to the actual reactor, which is discussed in detail in previous publications [21,32]. The reactor is basically a vertical tube in which the gases flow downwards and through a sintered quartz platform, where the sample is placed. To improve the efficiency of heating the samples a carbon susceptor surrounds the sample area. Samples can be placed within the susceptor hole (5 mm diameter) or on top, depending on whether or not they are porous. This system improves the infilling within the opals, over that obtained using a standard reactor, by both constricting the flow to a smaller area (22 mm diameter) and allowing gas to flow though any porous sample. Reactants used were trimethylindium ($1.9 \times 10^{-5}$ mol min$^{-1}$) (Epichem) with phosphine ($8.9 \times 10^{4}$ mol min$^{-1}$) (BOC) in a carrier gas of hydrogen (1 L min$^{-1}$). A cyclic method [33] is used in which the reactants are sequentially passed through the reactor to allow growth within the opal rather than on the surface. This cycle is repeated up to fourteen times, depending on the level of infill to be achieved. Prior to growth the samples are heated to 200 °C for 1 h to remove any moisture within the opal pores. During growth the organometalic is added at 50 °C and the phosphine at 400 °C at 30 min intervals.

Characterization was carried out via X-ray diffraction (Siemens D5000), micro-Raman spectroscopy (514.5 nm Ar line, Renishaw 1000), and SEM. The optical study was done by means of Bragg reflectance at normal incidence using a commercial Fourier-transform infrared (FTIR) spectrometer. In order to select regions of good quality, an optical microscope attached to the spectrometer was used. Zones of about 400 μm$^2$ were tested.

Received: June 7, 2004
Final version: July 30, 2004
Published online: December 20, 2004

[1] E. Yablonovitch, T. J. Gmitter, K. M. Leung, *Phys. Rev. Lett.* **1991**, *67*, 2295.
[2] S. John, *Phys. Rev. Lett.* **1987**, *58*, 2486.
[3] J. D. Joannopoulos, R. D. Meade, N. Winn, *Photonic Crystals. Molding the Flow of Light*, Princeton University Press, Princeton, NJ **1995**.
[4] R. Mayoral, J. Requena, J. S. Moya, C. López, A. Cintas. H. Míguez, F. Meseguer, A. Vázquez, M. Holgado, A. Blanco, *Adv. Mater.* **1997**, *9*, 257.
[5] C. López, *Adv. Mater.* **2003**, *15*, 1679.
[6] R. Biswas, M. M. Sigalas, G. Subramania, C. M. Soukoulis, K. M. Ho, *Phys. Rev. B* **2000**, *61*, 4549
[7] K. Busch, S. John, *Phys. Rev. E* **1998**, *58*, 3896.
[8] E. Palacios-Lidón, A. Blanco, M. Ibisate, F. Messeguer, C. López, J. Sánchez-Dehesa, *Appl. Phys. Lett.* **2002**, *81*, 4925.
[9] A. Blanco, E. Chomski, S. Grabtchak, M. Ibisate, S. John, S. W. Leonard, C. López, F. Meseguer, H. Míguez, J. P. Mondia, G. A. Ozin, O. Toader, H. M. van Driel, *Nature* **2000**, *405*, 437.
[10] H. Míguez, F. Meseguer, C. López, M. Holgado, G. Andreasen, A. Mifsud, V. Fornés, *Langmuir* **2000**, *16*, 4405.
[11] B. H. Juárez, M. Ibisate, J. M. Palacios, C. López, *Adv. Mater.* **2003**, *15*, 319.
[12] L. D. Zhu, K. T. Chan, D. K. Wagner, J. M. Baliantyne, *J. Appl. Phys.* **1985**, *57*, 5486.
[13] A. L.Reynolds, D. Cassagne, C. Jouanin, J. M. Arnold, *Synth. Met.* **2001**, *116*, 453.
[14] J. F. Galisteo-López, E. Palacios-Lidón, E. Castillo-Martínez, C. López, *Phys. Rev. B* **2003**, *68*, 115 109.
[15] P. Jiang, J. F. Bertone, K. S. Hwang, V. L. Colvin, *Chem. Mater.* **1999**, *11*, 2132.
[16] B. Gates, D. Quin, Y. Xia, *Adv. Mater.* **1999**, *11*, 466.
[17] M. Bardosova, P. Hodge, L. Pach, V. Smatko, R. H. Tredgold, D. Whitehead, *Thin Solid Films* **2003**, *437*, 276.
[18] Y. A. Vlasov, X. Bo, J. C. Sturm, D. J. Norris, *Nature* **2001**, *414*, 289.
[19] S. M. Yang, H. Míguez, G. A. Ozin, *Adv. Funct. Mater.* **2002**, *12*, 425.
[20] H. Miguez, S. M. Yang, N. Tetreault, G. A. Ozin, *Adv. Mater.* **2002**, *14*, 1805.
[21] H. M. Yates, D. E. Whitehead, M. G. Nolan, M. E. Pemble, E. Palacios-Lidón, S. Rubio, F. J. Meseguer, C. López, *Proc. Electrochem. Soc.* **2003**, *8*, 967.
[22] D. O. Henderson, A. Veda, Y. S. Tung, R. Mu, W. C. White, R. A. Zuhr, J. G. Zhu, *J. Phys. D* **1997**, *30*, 1432.
[23] H. M. Rietveld, *J. Appl. Crystallogr.* **1969**, *2*, 65.

  

ADVANCED FUNCTIONAL MATERIALS



[24] S. G. Johnson, J. D. Joannopoulos, *Opt. Express* **2001**, *8*, 173.
[25] F. García-Santamaría, M. Ibisate, I. Rodriguez, F. Meseguer, C. López, *Adv. Mater.* **2003**, *15*, 788.
[26] D. E. Aspnes, A. A. Studna, *Phys. Rev. B* **1983**, *27*, 985.
[27] J. C. Maxwell-Garnett, *Philos. Trans. R. Soc. London* **1904**, *203*, 385.
[28] V. Yannopapas, N. Stefanou, A. Modinos, *J. Phys. Condens. Matter* **1997**, *9*, 10 261.
[29] O. R. Monteiro, J. W. Evans, *J. Electrochem. Soc.* **1988**, *135*, 2366.
[30] F. Marlow, W. Dong, *ChemPhysChem* **2003**, *4*, 549
[31] W. Stöber, A. Fink, E. Bohn, *J. Colloid Interface Sci.* **1968**, *26*, 62.
[32] D. E. Whitehead, M. E. Pemble, H. M. Yates, A. Blanco, C. López, H. Miguez, F. J. Meseguer, *J. Phys. IV* **2002**, *12(Pr4)*, 63.
[33] H. M. Yates, M. E. Pemble, H. Míguez, A. Blanco, C. López, F. J. Meseguer, L. Vázquez, *J. Cryst. Growth* **1998**, *193*, 9.

  